Report on AWS radiance data quality

Brett Candy[1], Nigel Atkinson[1], Christina Köpken-Watts[2], Robin Faulwetter[2] and Anna Booton[1]

[1]Met Office, Exeter, United Kingdom
[2] DWD, Offenbach, Germany

This documentation was developed within the context of the EUMETSAT Satellite Application Facility on Numerical Weather Prediction (NWP SAF), under the Cooperation Agreement dated 7 September 2021, between EUMETSAT and the Met Office, UK, by one or more partners within the NWP SAF. The partners in the NWP SAF are the Met Office, ECMWF, DWD and Météo France.

Change record			
Version	Date	Author / changed by	Remarks
1.0	29/04/26	Brett Candy, Christina KW	First Version – Reviewed by Fabien Carminati

Contents

1. Introduction

The Arctic Weather Satellite (AWS) is an ESA mission which was launched on 16 August 2024. It is a small satellite that operates in a sun-synchronous low earth orbit (ascending node local time 22:38) and contains a microwave (MW) radiometer, the MWR, with both window and atmospheric sounding channels. The real time dissemination of the data is via EUMETCast Terrestrial. Consequently, use of the instrument is of considerable interest to NWP centres.

In addition to the conventional MW sounding channels for temperature (in the 50-60 GHz band) and water vapour (based around the 183 GHz line), the instrument also contains channels operating in the submm at 325 GHz. This is the first time that submm channels have operated on a low earth orbit satellite and this advancement allows the possibility of improved ice cloud detection and/or treatment of ice cloud or use of ice cloud information in all sky assimilation.

The AWS instrument also acts as a precursor to the planned EUMETSAT EPS Sterna constellation of up to six satellites in three orbits, with several studies (e.g. Lean et al., 2025) showing that the assimilation of data from such a constellation will yield large forecast impacts, even in the presence of measurements in the existing conventional satellite orbits. The quality assessment of the AWS observations is therefore important, as it is very likely that there will be other radiometers of a similar design operating soon.

Figure 1 shows six hours of orbit for AWS, and also compares the ground track for the operational AMSU instruments onboard Metop-B and Metop-C. The overpass times are quite close, with AWS ~30 minutes behind the Metop satellites. This improves data coverage in some regions, e.g. as seen over the Pacific Ocean in Figure 1.

In this report we present a quality assessment of the observations made by the AWS radiometer. The focus here is on the NWP perspective and we evaluate the instrument through comparing the observations with model equivalents from global NWP model short-range forecasts. By comparing the observations to a good quality estimate of the atmospheric state provided by state-of-the-art NWP models, data characteristics like scan biases can often be much more easily detected than in the raw data themselves. To compute the model equivalent observations, we use the EUMETSAT NWP SAF RTTOV fast radiative transfer model which is also widely used in operational NWP data assimilation systems. More details on RTTOV can be found in Saunders et al., 2018.

The quality assessment is done in an operational NWP framework and uses results from two NWP centres (UK Met Office and DWD) and looks at quality aspects as well as at data timeliness which is important especially for short-range NWP applications. This report is set out as follows: In Section 2 an overview of the instrument is presented as well as the pre-processing steps applied to the observations before use in NWP. In Section 3 the process by which the observations are compared to the model equivalents are discussed, this includes pre-screening of the data. Since the results come from two centres, there are differences in this process between the Met Office and DWD and both approaches are described. The comparisons are presented in Section 4. Section 5 looks at data timeliness and results of an initial impact study are presented in Section 6. Finally, conclusions are made in Section 7.

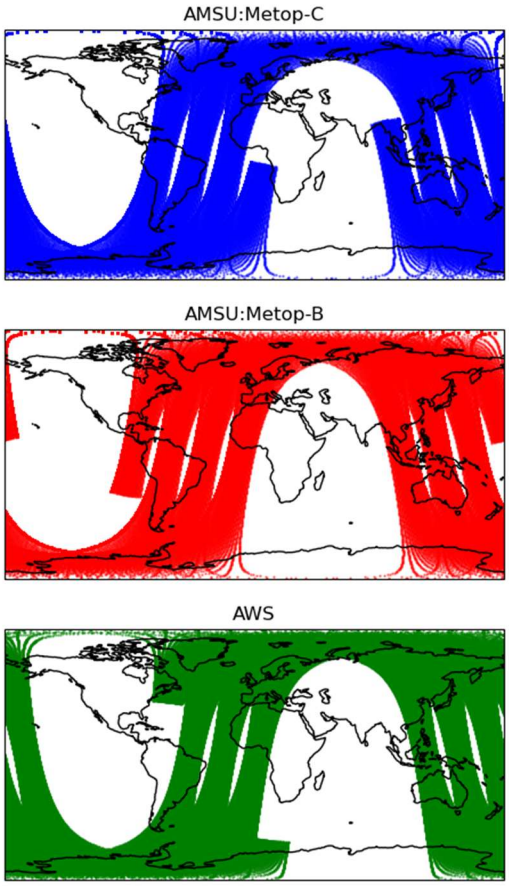

Figure 1: Spatial coverage plots for AMSU instruments on Metop-C and B compared to the AWS satellite. This is for six hours of data centred on 1st June 2025 at 12 UTC.

2. The AWS Instrument and pre-processing steps

The AWS instrument is a 19-channel cross-track microwave radiometer and was developed significantly faster than existing operational MW radiometers used in NWP (for example, the AMSU-A instrument). Also, it is smaller in size, with only 30kg mass compared to about 130kg for the MWS which will be flying on EPS-SG, which presents additional challenges for low noise measurements. The instrument contains four sets of receivers, covering channels around 54, 89, 174 and 325 GHz respectively (Eriksson et al., 2025). The channel characteristics are shown in Table 1. The NEdT values given in Eriksson et al., 2025, correspond to integration times of 10ms, 5ms, 2.5ms and 2.5ms for the four bands, for consistency with the instrument specification; they are not single-sample NEdTs.

Channel	Feedhorn Group	Frequency (GHz)	Footprint (km)	NEdT (K)
1	1	50.300	40	0.32
2		52.800	40	0.21
3		53.246	40	0.25
4		53.596	40	0.22
5		54.400	40	0.22
6		54.940	40	0.29
7		55.500	40	0.38
8		57.290	40	0.90
9	2	89.000	20	0.14
10	3	165.500	10	0.27
11		176.311	10	0.39
12		178.811	10	0.42
13		180.311	10	0.58
14		181.511	10	0.66
15		182.311	10	0.81
16	4	325.150±1.2	10	1.44
17		325.150±2.4	10	1.53
18		325.150±4.1	10	0.95
19		325.150±6.6	10	0.80

Table 1: AWS radiometer channel characteristics. The instrument noise, expressed as NEdT, are taken from Eriksson et al., (2025) using inflight data. All channels have a QV polarization.

Channels 1 to 8 provide temperature sounding in the troposphere to lower stratosphere, and Channels 10 to 15 provide water vapour sounding in the troposphere. Channel 9 is a window channel and can be used as part of screening for precipitation in the field of view (e.g. Bennartz, 2002). The final feedhorn contains a set of four channels centred around the 325 GHz water vapour line. This is the first time that channels in the submm part of the microwave spectrum have been used on an instrument targeted for operational NWP use. It is expected that these channels will be more sensitive to scattering by ice hydrometeors than the 183 GHz channels.

Compared to existing instruments such as the Advanced Technology Microwave Sounder (ATMS), AWS does not include the high-altitude temperature sounding channels in the 50 - 60 GHz band, nor does it include the low frequency channels operating below 50 GHz. This is a design choice to reduce complexity.

Another feature of the AWS design is that the angle between the main antenna and each feedhorn is slightly different. This results in each feedhorn having a different cross track scan pattern on the ground as is shown in Figure 2. The overall swath width is about 1870 km with a maximum scan angle of 54.4°.

Data are downlinked from the satellite once per orbit to the Svalbard satellite station, processed at ESA, transmitted to EUMETSAT and then arrives at European NWP centres via EUMETCast Terrestrial. For Nowcasting and short-range NWP applications there is also a direct broadcast transmission. The results shown in this report are from the global data records obtained via the EUMETCast service after this has been setup in mid-April 2025. Starting on 13th March 2025, an antenna pattern correction is applied in the ESA processing. Since the observations from the various feedhorns are not collocated geographically the first step in the pre-processing at both DWD and UK Met Office is to perform a remapping of the

observations from each feedhorn onto the same location. This is performed by an AWS module in the EUMETSAT NWP SAF AAPP software (referred to in this report as AAPP-AWS), with the data from feedhorns 1,2 and 4 being remapped onto the horn 3 (frequencies 166 – 182.311 GHz) swath locations. The observations are also highly oversampled (meaning successive footprints across the swath overlap) and so spatial averaging is also applied using AAPP-AWS, followed by spatial thinning. The amount of averaging varies between the two centres; at Met Office a 3x3 average is performed and then the resulting data is thinned by taking 1 in 3, whereas at DWD the averaging is a 5x5 average. The incoming level 1b files have 145 samples per scan; this is reduced to 49 in the Met Office processing. Figure 3 shows the resampled and averaged data for Met Office pre-processing for the same location as the raw data in Figure 2.

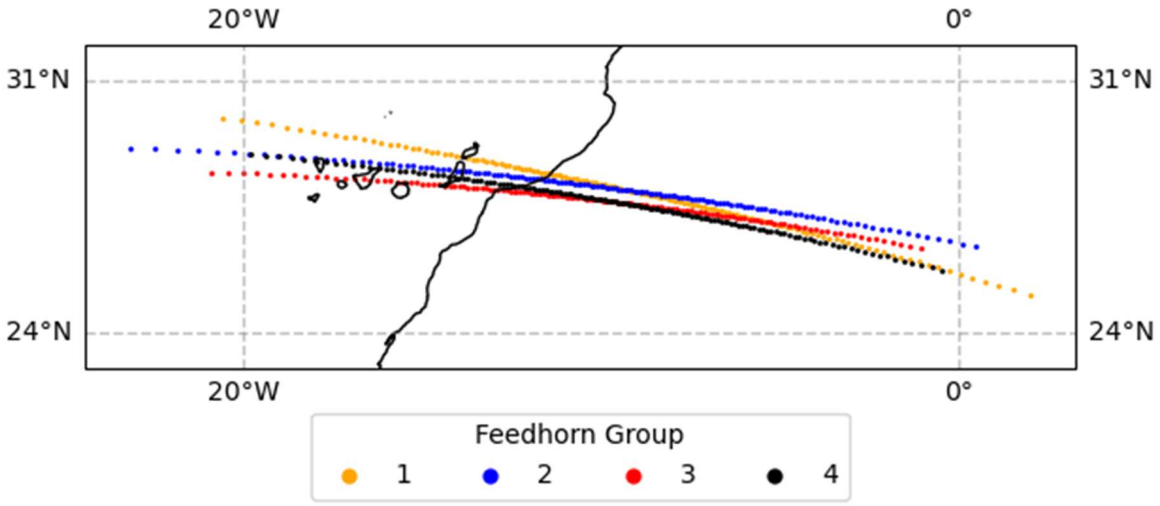

Figure 2: An example of the ground location of each Feedhorn Group for the same cross scan. The location is over the coast of Africa and the satellite is in descending node.

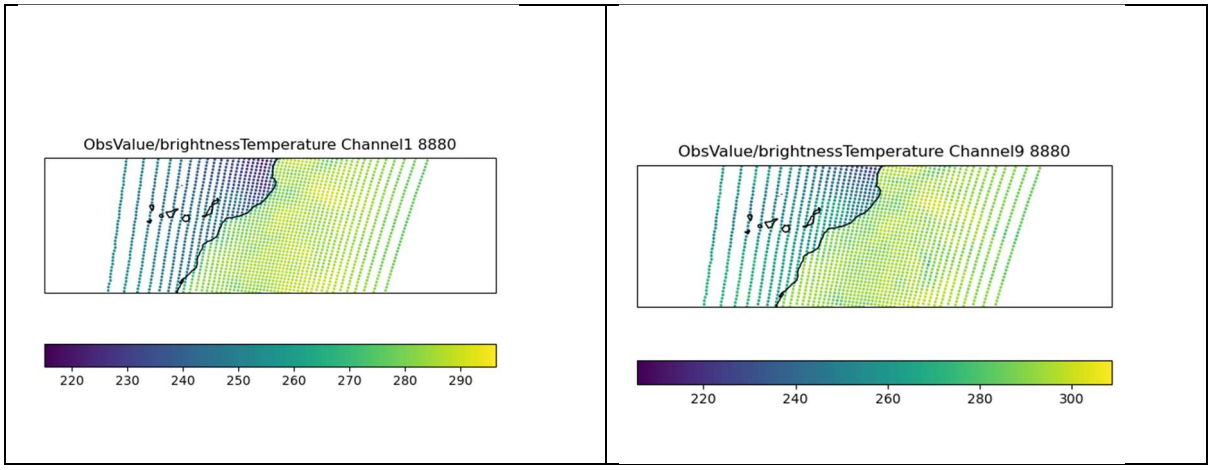

Figure 3: An example of the remapped and spatially averaged data using AAPP-AWS for two different feedhorns – *Left panel:* Channel 1, *Right panel:* Channel 9, The region is the same as in Figure 2.

The submm channels in Feedhorn 4 are based around the water vapour line at 325 GHz. The weighting functions for these channels are compared to the channels in Feedhorn 3 which operate at lower frequency close to the 183 GHz line. (channels 11-15) in Figure 4. The altitudes of peak sensitivity are very similar for these two channel sets, noting that channel 11 peaks lower than any of the channels in Feedhorn 4.

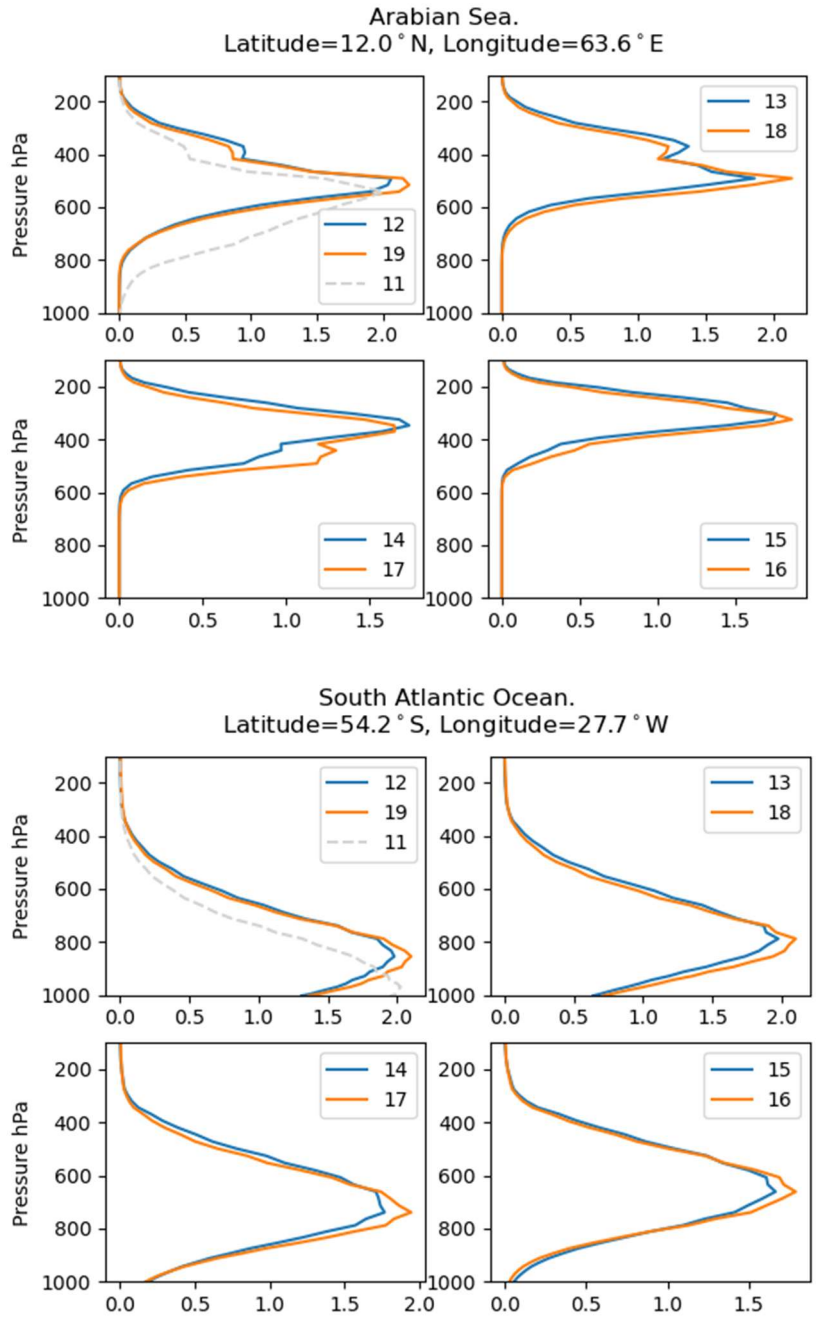

Figure 4. A comparison of the Weighting Functions derived from RTTOV simulations for 183 GHz channels (11-15) and 325 GHz channels (16-19) operating on AWS. The top panels are for a Tropical profile (in the Arabian Sea) and the bottom panels are for a mid-latitude profile (South Atlantic).

Whilst the peaks of the weighting functions for the 183 GHz and 325 GHz are very similar, the scattering effect of ice hydrometeors is much stronger in the higher frequency band; the ability to detect and retrieve ice cloud information was one of the prime motivators in adding this new band to the instrument (Eriksson et al., 2025). A good demonstration of this can be seen in Figure 5 where AWS made an overpass of the category 5 Hurricane Melissa. This data, which is averaged and thinned using the Met Office 3x3 approach shows considerably more scattering in the vicinity of the cyclone in the 325 GHz band. It is apparent in all of the channels in this band, even for channel 16 which peaks highest in the troposphere. For instance, channel 19 has a minimum brightness temperature of 119 K, which corresponds to a reduction due to scattering from hydrometeors of around 150 K.
As noted, Figure 5 is formed from averaged data. The corresponding Figure from the raw (without remapping or averaging) data can be seen for channel 19 in Figure 6. The raw data shows a minimum temperature of 111 K and the eye of the cyclone is very clear.

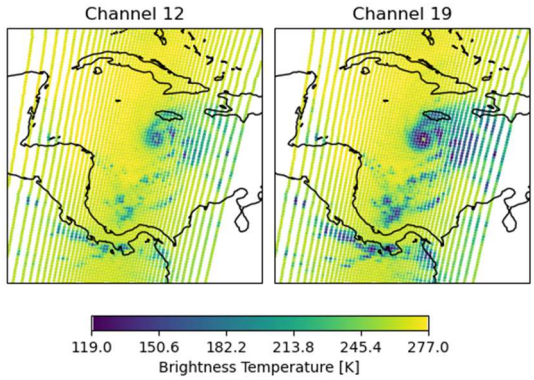
Channel 12
Channel 19
119.0 150.6 182.2 213.8 245.4 277.0
Brightness Temperature [K]

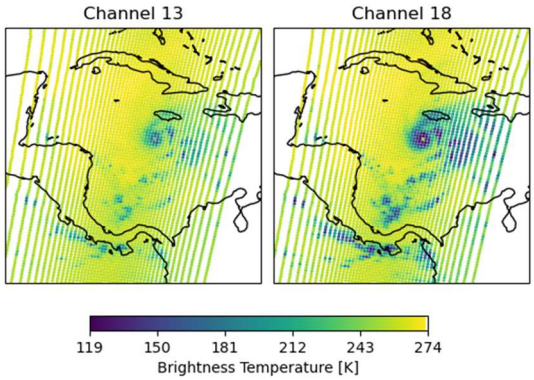
Channel 13
Channel 18
119 150 181 212 243 274
Brightness Temperature [K]

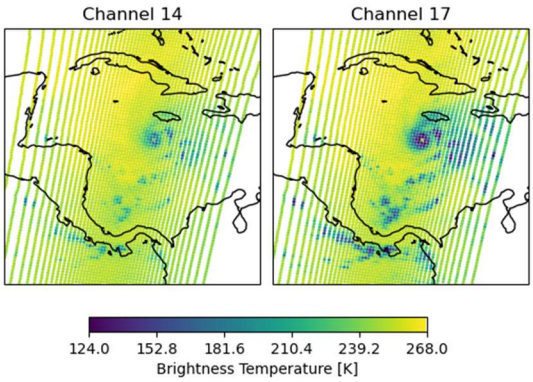
Channel 14
Channel 17
124.0 152.8 181.6 210.4 239.2 268.0
Brightness Temperature [K]

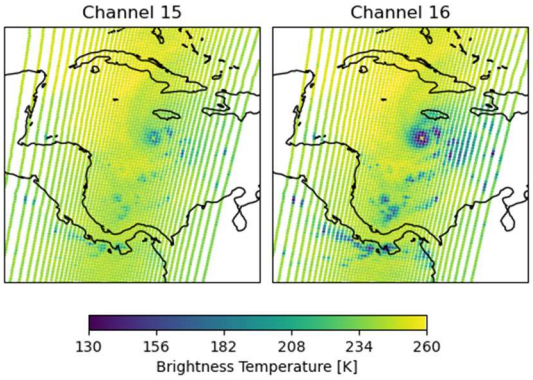
Channel 15
Channel 16
130 156 182 208 234 260
Brightness Temperature [K]

Figure 5: AWS 183 GHz channels (left panel) and corresponding 325 GHz channels (right panel) in the vicinity of Hurricane Melissa. The overpass date and time is 27th October 2025 at 15:50:32 UTC.

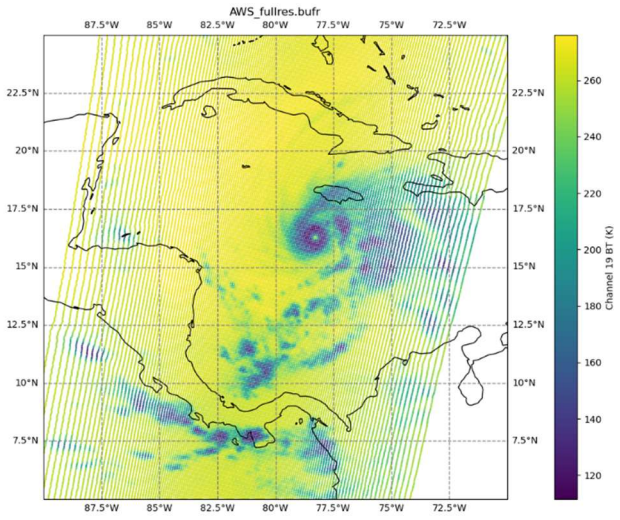

Figure 6: AWS 325 GHz channel 19 in the vicinity of Hurricane Melissa. The overpass date and time is as Figure 5 but instead is a plot of the raw observations.

3. Data Screening, Radiative Transfer and Bias Correction

3.1 AWS data screening

Since the aim here is to evaluate the quality of the instrument measurements with respect to NWP model equivalent brightness temperatures, the dataset needs to be screened for scenes that are difficult to model, either through complexities in the radiative transfer or in the underlying NWP model. For these reasons the data screening removes data over complex surfaces and where significant cloud is in the field of view. Due to the differing operational configurations at the two NWP centres the tests employed for data screening vary and are described for each centre in turn below.
At the Met Office the following screening tests are employed (based on those described in Candy and Migliorini, 2021):

- Data is over land or sea-ice – all channels rejected
- Channel specific screening is applied in the following way:
    - Rain in field of view (following Bennartz et al., 2002): all channels screened out
    - Significant ice hydrometeors in field of view as specified by a cost test of 183 GHz channels: channels 10-19 screened out
    - Low level cloud test using channel 2 departures: channels 1-4, 9-11, 19 screened out

A 1D-Var minimisation is then performed at each location with at least one channel remaining after the screening. This must successfully converge.
At DWD the following screening tests are employed:

- Data over sea and land are included, but over land with high model orography (higher than 1000m) all channels are rejected.
- Coastal points are excluded based on the size of the FOVs and a high resolution land-sea mask (MERIT-REMA topography used on a regular 10km resolution grid)
- QC for temperature channels (50GHz band, channels 1-8):
    - LWP retrieval (following Qin/Zou, 2016) > 1.2: channels 1-8 rejected (This is a temporary approach, a LWP retrieval currently being re-fitted using dedicated radiative transfer simulations for AWS)
    - Over land and sea-ice: channel 2 abs(O-B) > 1.2 K: channels 1-8 rejected
- QC for water vapour channels (183GHZ and 325GHZ, channels 9-19):
    - channel 10 abs(O-B) > 2.5 K: channels 9-19 rejected
    - TB(channel 11) – TB(channel 15) < threshold or channel 15 < threshold: channels 9-19 rejected (following cloud check by Buehler et al., 2007) (the thresholds are scan angle and latitude dependent)

With respect to the forward operator, both centres interpolate the model fields from its grid to the centre position (latitude, longitude) of the satellite field-of-view (FOV) and apply radiative transfer modelling to compute model equivalent radiances and brightness temperatures for all AWS/MWR channels. The radiative transfer model used is the fast model RTTOV. The versions of RTTOV differ, due to the respective current operational configurations at each centre. The Met Office uses version 12.3 whilst DWD uses version 13.2. The fast model coefficients for the MWR sensor have been trained on line-by-line simulations using the AMSUTRAN model (Turner et al., 2019), taking into account the measured spectral response functions for the instrument. At the Met Office, the RTTOV option to use the model cloud liquid water contents in the forward calculations is used.

The emissivity model used in the RTTOV simulations over sea is FASTEM 6 at the Met Office and also at DWD. For FOVs over land DWD uses an emissivity retrieval based on the observed TBs of Channel 1 (following Karbou et al, 2005) along with the TELSEM MW2 emissivity atlas provided within RTTOV as a fall back.

3.2 ATMS data pre-processing and data screening

ATMS data are used for comparing the results of the new AWS/MWR to a well-established instrument used operationally in NWP. The ATMS data are taken from the NOAA-20 instrument. The Met Office applies an averaging as detailed in Doherty et al., 2015, and at DWD ATMS data are averaged over 3*3 ATMS FOVs. This results in a broadly comparable, but not identical resolution to AWS/MWR.
The quality checks applied per band are similar in approach as now adapted for AWS/MWR, but with different thresholds to take different channel characteristics and instrument noise into account. Therefore, this comparison is intended to provide a context to the magnitude of the deviations found for AWS with respect to operational usage of a similar instrument in NWP and is not meant as a strict channel-per-channel comparison to evaluate instrument noise as such.

3.3 Bias correction

The algorithms used in NWP data assimilation systems assume unbiased observations and model. However, in reality neither of them are truly bias free. Satellite observations in the

MW range e.g. frequently display an instrument scan angle dependency in biases and sometimes orbital biases. Biases, contributing to the channel dependent biases, are also present both in the corresponding NWP fields and in the used forward operator, i.e. the radiative transfer. Therefore, a bias correction is generally applied in NWP before assimilation and approaches differ depending on the NWP centre specific implementations. At the Met Office the initial bias correction procedure for each channel removes the-cross scan variation and any remaining residual bias as a constant term. This is updated once per month during the monitoring period. Once this is done a more complex bias correction is used in the assimilation runs including terms that depend on the airmass (see link below for further details).
At DWD, a similar two-step approach is implemented using first a scan bias correction removing the average scan position dependent biases and secondly a situation dependent bias correction based on a linear regression with predictors derived for each atmospheric model profile from the NWP model fields. Both the scan correction and the airmass dependent correction components are based on long statistics and automatically updated online using the data from each 3h assimilation cycle.
Details on the methods implemented at the different centres are described in the summary provided on the NWP web page, see: Monitoring and bias correction | NWP SAF

4. Results

4.1 Introduction

The following sections show results of the observation minus first guess differences from each NWP centre, after data has been screened for scattering and/or absorption due to hydrometeors and complex surfaces as described in section 3.1. The results are accumulated over a three-month period starting on 20th March 2025 after the antenna correction began to be applied to the data on 13th March 2025 in the ESA processing. It is also worth noting that from mid-April the data was received via the EUMETCast service, while the first weeks were distributed via a dedicated ftp access for institutes supporting the CalVal effort.
The time series of data extracted from the Met Office database for each 6-hour cycle in the 3-month monitoring period is shown in Figure 7. This is after processing through AAPP-AWS and so includes data thinning (by 1 in 3). The time series shows very good data availability from the AWS instrument with only two periods of outage (2025-05-05 to 2025-05-13 and 2025-06-15 to 2025-06-20). There are several events in the time series where the amount of data doubles. This was investigated and the dataset at these times is a duplicate. We believe that this is an artefact of the storage in the Met Office database, rather than a dissemination issue.
For details on current data numbers and data timeliness, please see Section 5.

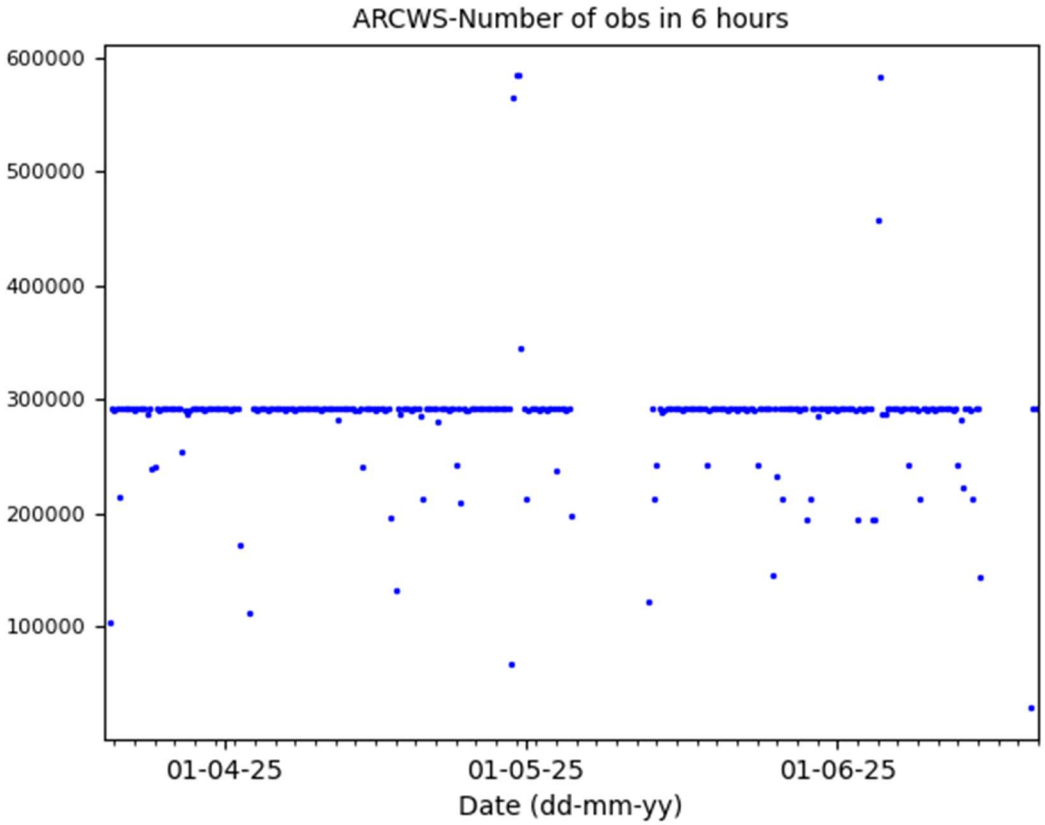

Figure 7: Time series of number of AWS observations after the remapping step used at the Met Office (i.e. number of FOVs after spatial averaging and 1 in 3 thinning) available in 6-hour intervals within the Met Office observation database during the Monitoring period. The data has been pre-processed through AAPP-AWS.

4.2 Analysis of Cross Scan Bias

Figures 8 to 10 show the cross scan mean value of the observation minus first guess difference (prior to the application of bias correction) for each of the sets of sounding channels. In each case the top panel show results from DWD and the lower panel from the Met Office. In practice for most microwave instruments which operate using a cross-track scanning geometry we find that the bias varies with the spot (or scan) position. The reasons for this include errors in the antenna corrections or in the assumed channel passbands (e.g. as discussed in Lupu et al., 2016). For the AWS channels this is also the case. Although the absolute biases may differ, e.g. due to slightly different biases in NWP model humidity profiles, results from both centres show similar variations across the spot position. Some differences in slope, e.g. in the 325 GHz band channels, may also be linked to different approaches in the applied quality checks (detection of scattering signal) and are under further investigation. The cross-scan bias patterns are generally very stable in time (not shown). Channels in Feedhorn groups 1 and 3 appear to have a cross-scan variation that is asymmetric, with Feedhorn 3 channels exhibiting a much stronger asymmetry. The channels operating near the 183 GHz water vapour line (channels 11-15) exhibit a strong positive slope in the bias with scan position which is clearly visible in the monitoring at both NWP

centres. (see Figure 9). These results can also be derived for existing cross track radiometers such as the ATMS instrument onboard NOAA-20. We find that in general the AWS instrument has larger cross scan asymmetry in the bias than for ATMS in both the 50 GHz band (see Figure 11) and also for the 183 GHz band (Figure 12).
ESA have investigated the surprisingly strong scan dependency in the Feedhorn 3 channels and believe that it is due to a small particle of debris in the feedhorn. The particle temperature, and subsequently its thermal emission, cycles as the antenna rotates. Despite this relatively large variation in cross track bias for AWS data, it appears to be stable with time and consequently NWP bias correction schemes should be able to remove it. That the bias correction indeed is well able to handle and remove the across scan bias efficiently can be seen in Figures 8-10 in the DWD monitoring plots with the dashed lines showing the residual bias once a bias correction has been applied to the brightness temperatures.

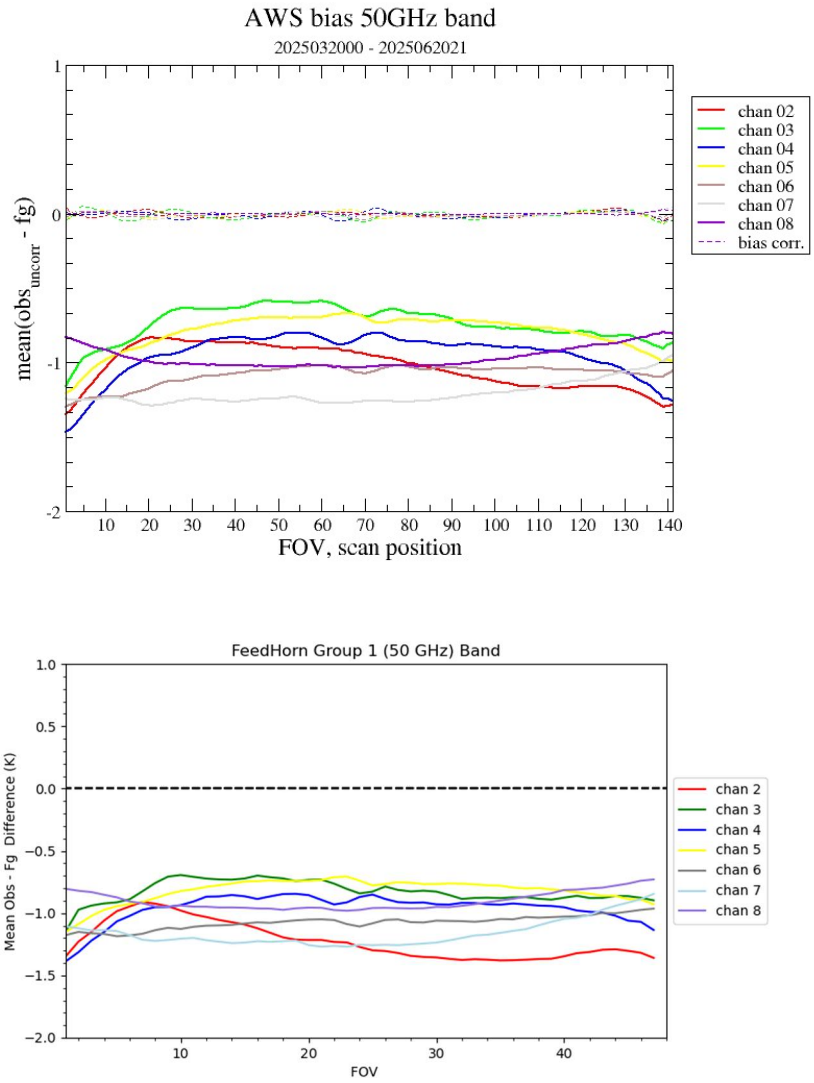

Figure 8. Cross scan O-B difference for sounding channels 2 to 8 in the 50 GHz band, Feedhorn Group 1. The *top panel* is from DWD monitoring, the *bottom* one from Met Office monitoring. The corresponding Corrected-Background (C-B) statistics are shown in the DWD plot as dashed lines.

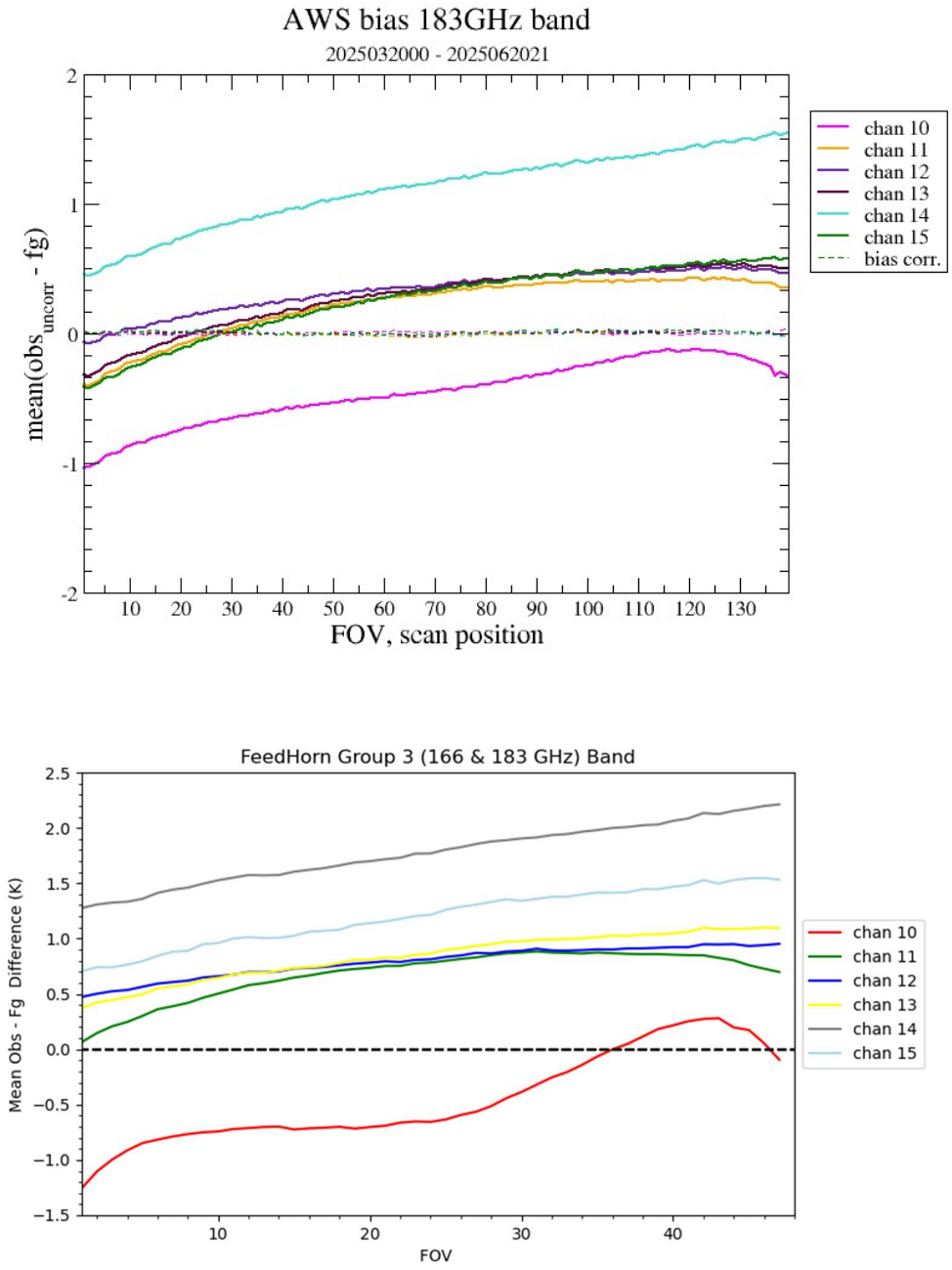

Figure 9. Cross scan O-B difference for humidity sounding channels 10 to 15 in the 166 GHz channel and the 183 GHz band, Feedhorn Group 3. The *top panel* is from DWD monitoring, the *bottom* one from Met Office monitoring.

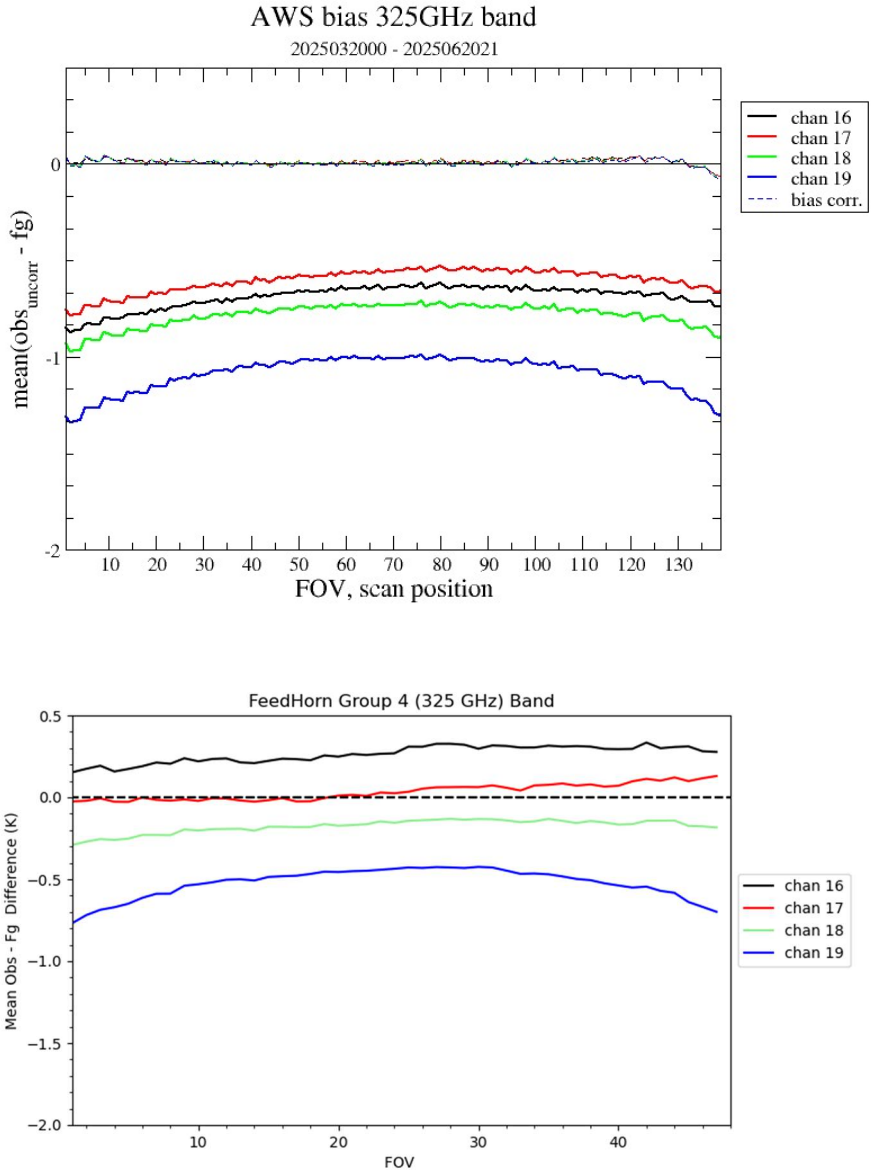

Figure 10. Cross scan O-B difference for humidity sounding channels 16 to 19 in the new 325 GHz band, Feedhorn Group 4. The *top panel* is from DWD monitoring, the *bottom* one from Met Office monitoring.

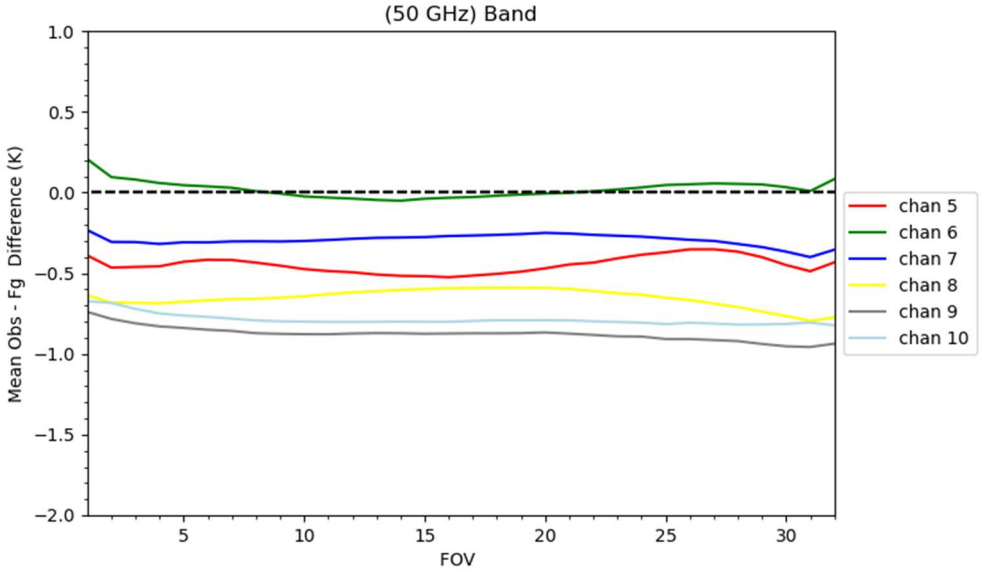

Figure 11. Cross scan O-B difference for 50 GHz channels from NOAA-20 ATMS. This is from Met Office monitoring.

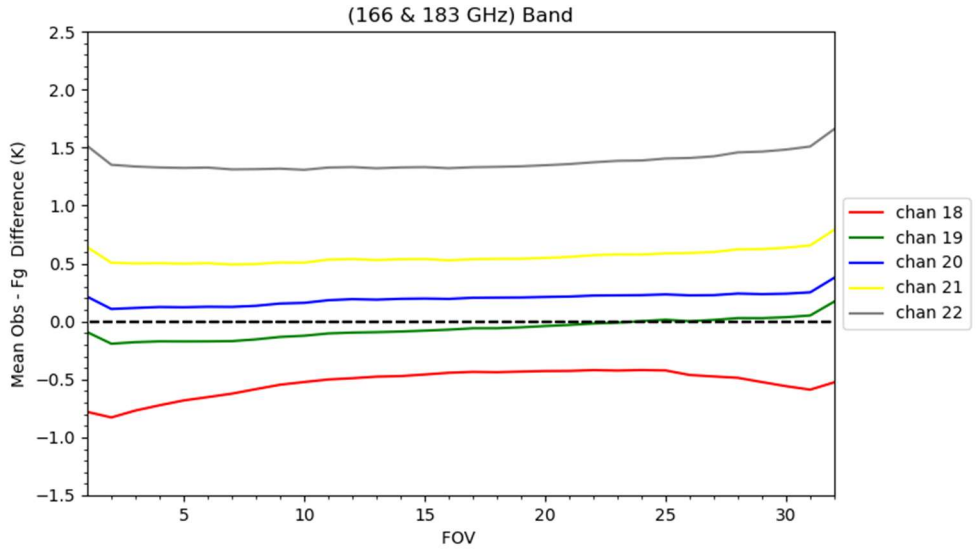

Figure 12. Cross scan O-B difference for 183 GHz channels from NOAA-20 ATMS. This is from Met Office monitoring.

4.3 Time series of Observation minus first guess differences

In the following results (Figures 13 – 15) we look at the temporal stability of the MWR/AWS observations showing timeseries of statistics for observations minus background (named O-B) as well as corresponding results after a bias correction has been applied (named C-B) to the AWS brightness temperatures as described in Section 3.3.
The average biases of the uncorrected data (see top panels in Fig. 13-15) are very stable in time, showing only very minor variations that are very likely linked to changes in meteorological conditions and geographical area covered between the different analysis cycles. This highlights that the instrument does not show any large instabilities in terms of measurement quality. A very small more systematic step change of less than 0.1 K in mean bias is detected for the channels in the 50 GHz band around 9 April 2025 in both the Met Office and DWD monitoring. However, the NWP bias correction adjusts and is able to correct biases of C-B back to zero after a few days (see e.g. top panel Fig. 13).
For all channels, the residual biases after bias correction appear very small and do not vary greatly through the timeseries. Likewise, the standard deviation of the observations minus background (before and after bias correction) is also very stable in time for all channels and in all frequency bands (not shown).

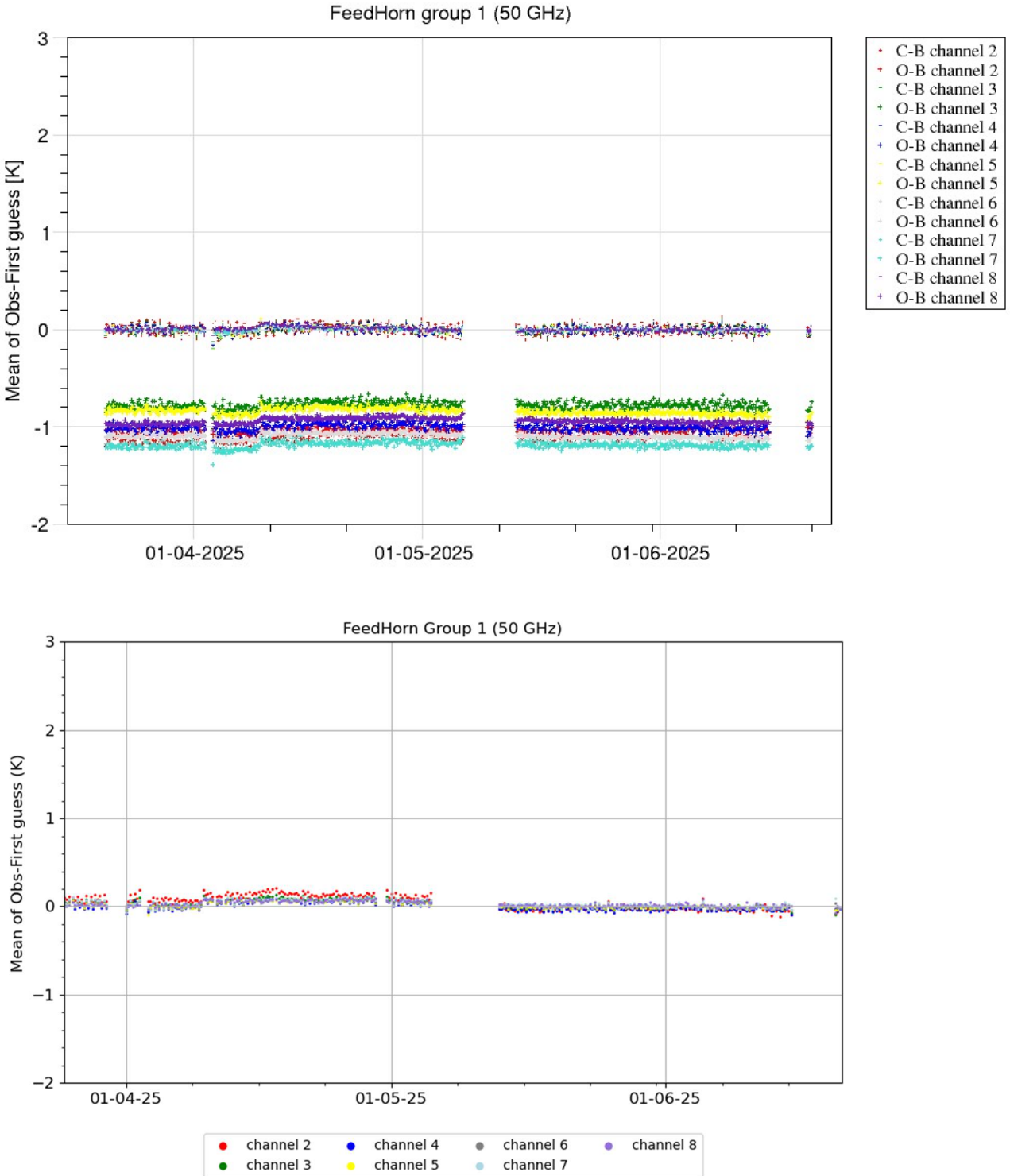

Figure 13. Time series of O-B and C-B difference (after bias correction has been applied) for channels 2 to 8 in the 50 GHz band, Feedhorn Group 1. The *top panel* is from DWD monitoring (including departure statistics for both uncorrected, O-B, and bias corrected, C-B, observations), the *bottom panel* from Met Office monitoring (C-B only).

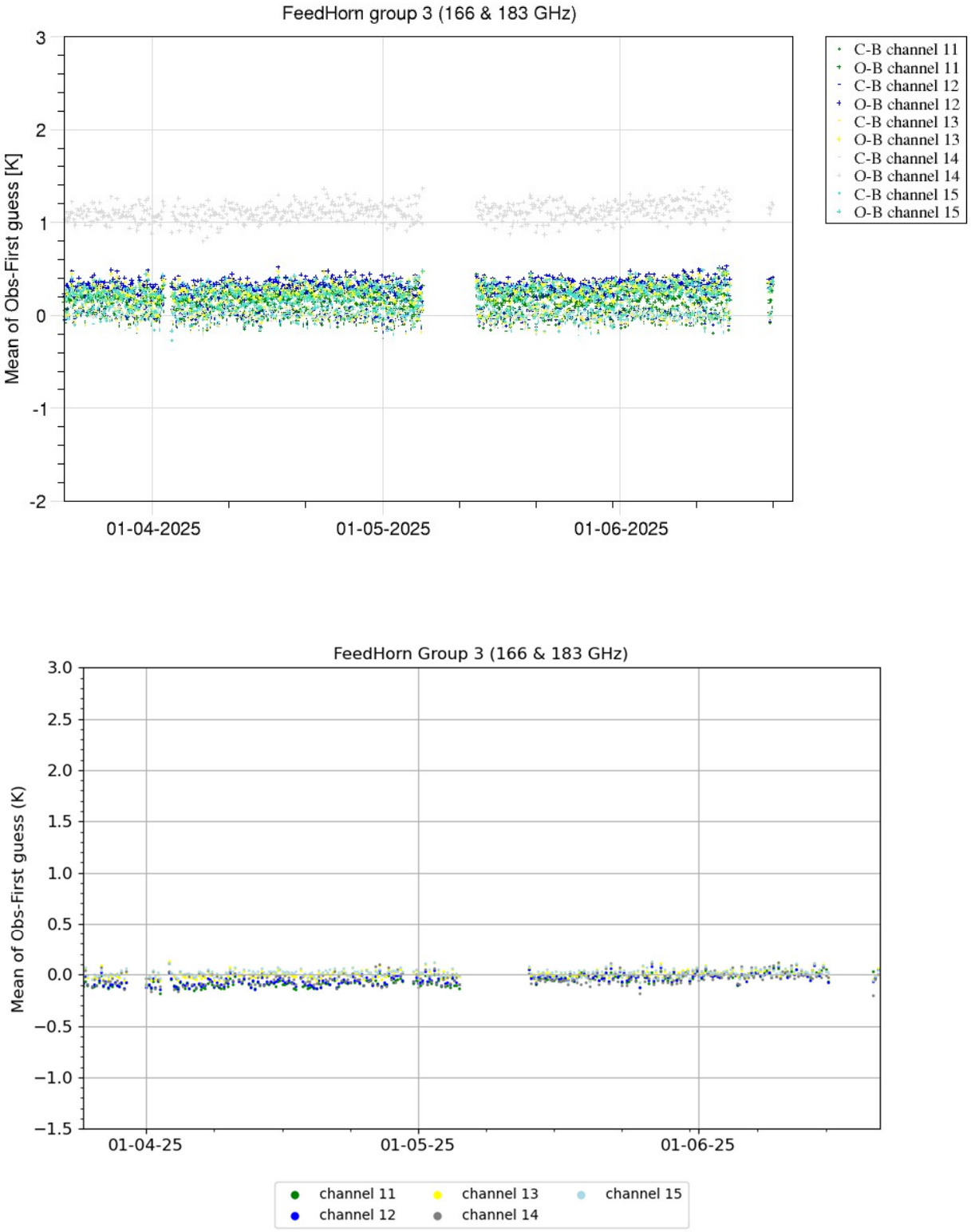

Figure 14. As in Fig 12, but for channels 11 to 15 in the 183 GHz band, Feedhorn Group 3. The *top panel* is from DWD monitoring, the *bottom panel* from Met Office monitoring.

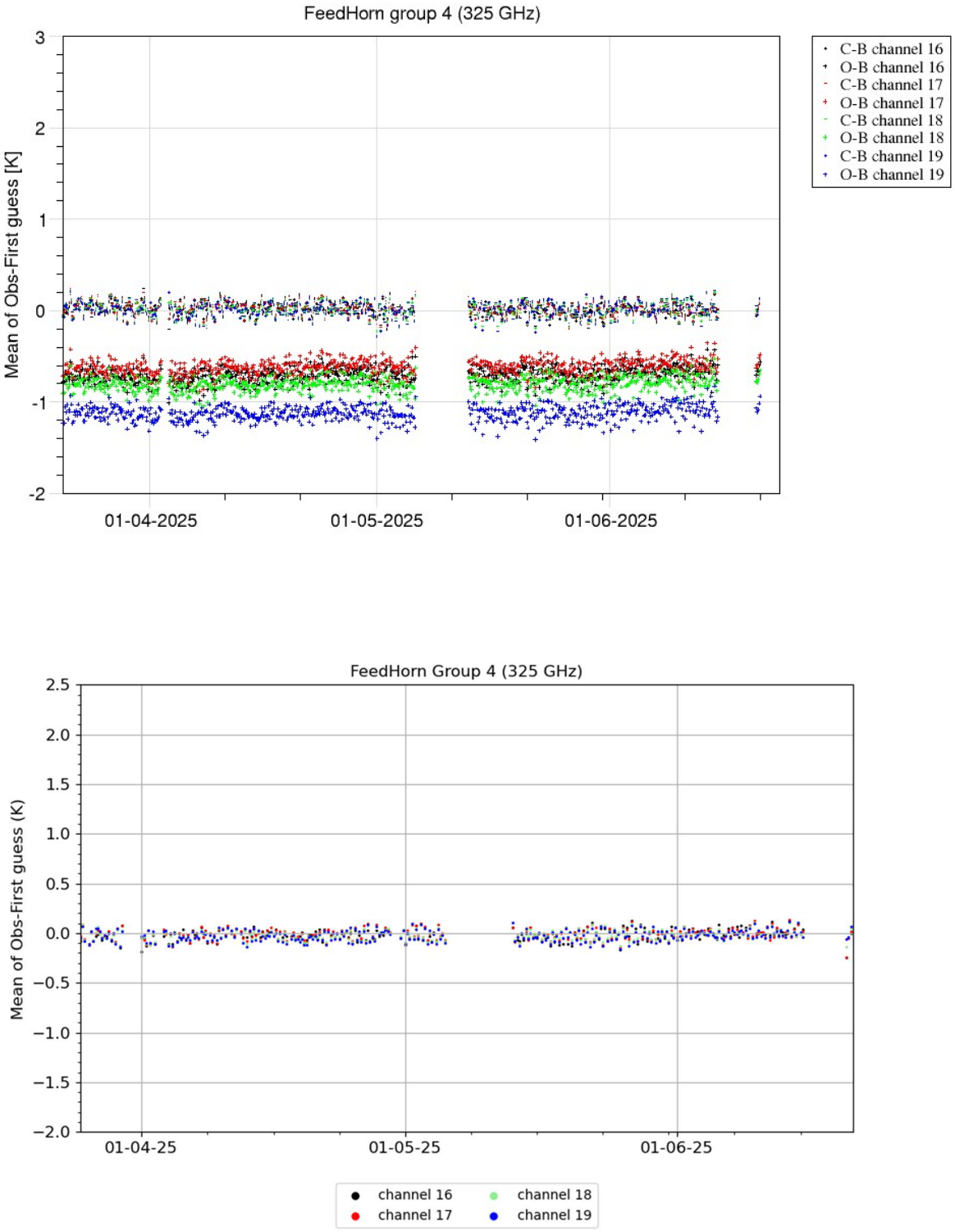

Figure 15. As in Fig. 12, but for channels 16 to 19 in the 325 GHz band, Feedhorn Group 4. The *top panel* is from DWD monitoring, the *bottom panel* from Met Office monitoring.

4.4 Assessment of the instrument noise

In this section we look at the distribution of the observation minus first guess departures after bias correction has been applied (we refer to this as 'corrected minus background', C-B). These differences include contributions due to instrument noise, but also random errors of the NWP model background and forward model (mostly radiative transfer) as well as representativeness errors, e.g. due to resolution and collocation mismatch between observation and model grid point values. Systematic errors of the observations, the NWP model and the radiative transfer forward model are corrected for through the applied bias correction as discussed above.
Table 2 shows the standard deviation of this metric for each AWS channel from both centres. Also shown as a reference, is the standard deviation for C-B from ATMS channels with the same central frequency.

AWS channel & Frequency (GHz)	**Standard Deviation C-B (K) ATMS equivalent channels in brackets**		**NEdt (K)**
	DWD	**Met Office**	
2: 52.800	0.39	0.438	0.21
3: 53.246	0.268	0.275	0.25
4: 53.596	0.204	0.240	0.22
5: 54.400	0.16 [0.117]	0.211 [0.106]	0.22
6: 54.940	0.172 [0.123]	0.266 [0.107]	0.29
7: 55.500	0.213 [0.142]	0.355 [0.118]	0.38
8: 57.290	0.4 [0.169]	0.698 [0.148]	0.90
10: 165.500	0.885 [1.883]	1.547 [1.511]	0.27
11: 176.311	1.086 [1.065]	0.820 [0.801]	0.39
12: 178.811	1.202 [1.185]	0.930 [0.766]	0.42
13: 180.311	1.327 [1.391]	0.851 [0.807]	0.58
14: 181.511	1.474 [1.480]	1.183 [0.881]	0.66
15: 182.311	1.632 [1.629]	0.923 [0.978]	0.81
16: 325.150±1.2	1.583	1.400	1.44
17: 325.150±2.4	1.5	1.415	1.53
18: 325.150±4.1	1.422	1.097	0.95
19: 325.150±6.6	1.379	1.051	0.80

Table 2: The standard deviation of the observation minus first guess departures is given for values after bias correction has been applied. Results are shown for AWS from the monitoring statistics at both centres. As a comparison the numbers in brackets show the same metrics for ATMS channels (NOAA-20) which have similar channel characteristics. The right column gives the NEdT values of AWS/MWR according to Eriksson et al., (2025) using inflight data.

It can be seen in Table 2 that most of the temperature sounding channels (Feedhorn 1) have a standard deviation (stdv) of C-B in the range 0.2 – 0.3 K and results between the two centres are overall very consistent. A revision of the used QC at DWD which is currently ongoing leads to slightly larger stdv(C-B) with marginally larger values and closer to the Met Office results. The difference in the stdv(C-B) from the two centres for AWS channel 10 is most likely due to differing QC procedures for this channel.
The stdv values for AWS are larger than for the corresponding ATMS channels but within the range considered to be beneficial in NWP data assimilation (e.g. from Kalluri et al. 2021).

Also, these deviations remain significantly smaller than in the specification of the instrument (see WMO-OSCAR at https://space.oscar.wmo.int/instruments/view/mwr_aws) which is an excellent result, especially given the small size of the instrument and satellite compared to ATMS.

The standard deviation in C-B for channel 8 of AWS stands out in the monitoring results of both Met Office and DWD as significantly higher than for the other channels of the 50 GHz band. As it is also much higher than the values for the corresponding ATMS channel, this points to a significantly higher instrument noise in channel 8. This result is consistent with a known issue of the instrument (ESA communication).

The standard deviation in C-B for the AWS water vapour channels in the 183 GHz band is in the range 0.8 to 1.2 K for the Met Office, but slightly higher at DWD with a range of 1-1.6 K. The results are consistent with a higher instrument noise in this range according to specifications. Additionally, C-B deviations for humidity sensitive channels generally contain larger representativeness error components due to small scale variations in humidity which are not necessarily fully represented by the NWP models. This effect contributes more strongly at DWD, as with the relatively short 3h steps used in the NWP assimilation cycling a time interpolation of the first guess is currently not applied. For the corresponding ATMS channels at 183 GHz the C-B statistics have very similar values which supports this explanation.

The new submm channels in the 325 GHz band have overall slightly larger errors than those in the 183GHz band but still in a similar range. Both the 183 GHz band and the new 325 GHz band are in the range considered beneficial in NWP data assimilation (based on Kalluri et al, 2022 and from experience with existing instruments).

Figure 16 illustrates the effect of the FOV averaging (superobbing) on the comparison results, showing standard deviation of C-B differences computed for the individual observations as well as for the 5*5 averages. As expected, the statistics for individual FOVs show larger deviations to the model due to higher noise components in individual measurements than in superobbed data. This effect is more pronounced for the temperature sounding channels (nos. 2-8) in the 50 GHz band than in the 183 and 325 GHz bands, where representativeness and radiative transfer inaccuracies contribute a larger component of the observation to model comparison.

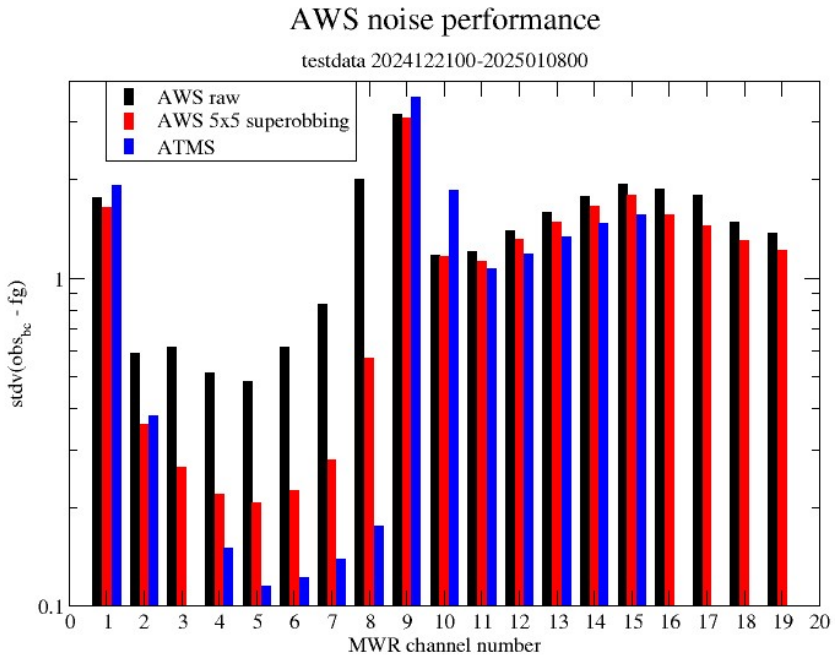

Figure 16: Standard deviations of C-B based on DWD results for MWR data with full resolution (as output from AAPP-AWS interpolated on feedhorn 3, black bars) and for the 5*5 averages used in the overall results of this report (red bars) together with results for ATMS (3*3 averages, blue bars).

Figures 17 and 18 show histograms of the C-B differences for a temperature sounding channel and a water vapour sounding channel (in the 183 GHz band). Both show a distribution that generally follows approximately a Gaussian distribution. Note that the warm tail in the Met Office results for the water vapour channel (Fig. 18) is an artefact of the cloud tests and distribution for the corresponding ATMS channel has a similar characteristic (not shown). The other channels in the temperature and water vapour sounding bands display similar distributions again underlining that MWR/AWS observations are well suited for active assimilation in NWP. In particular, we also see a Gaussian distribution for the new submm channels (Figure 19).

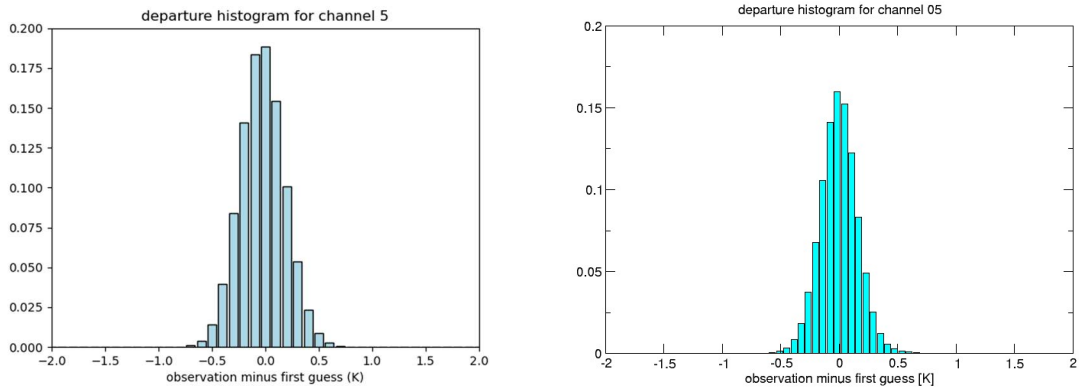

Figure 17. Normalised histograms of the Observation minus first guess difference (after bias correction, i.e. C-B) for AWS channel 5 for Met Office results (left) and DWD results (right).

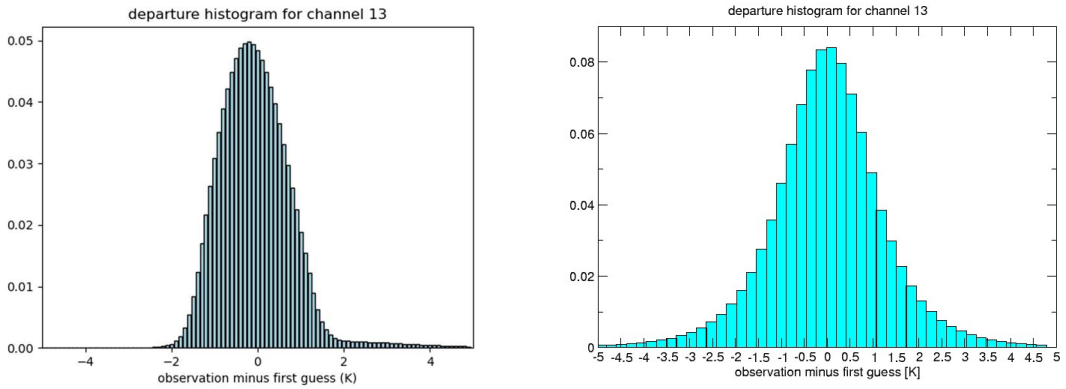

Figure 18. As in Fig. 16 but for AWS channel 13.

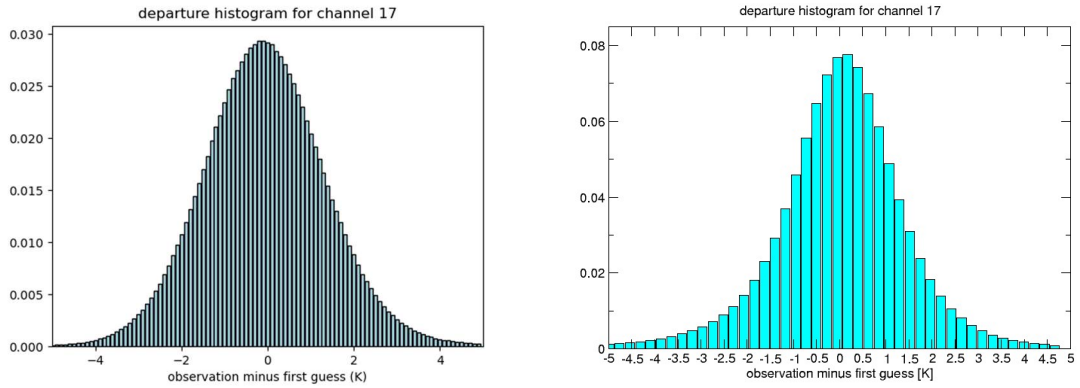

Figure 19. As in Fig. 16 but for AWS channel 17 (325.150±2.4 GHz).

4.5 Assessment of Striping Noise

Striping noise has been detected in several operational microwave radiometers. These include ATMS on Suomi NPP, notably in the 50 GHz channels (Doherty et al., 2015) and the 157 GHz channel on Metop-A MHS (Yang et al., 2021). This form of noise manifests as striping in the along track direction in the radiance data, but generally is clearly detected in spatial maps of the observation minus first guess difference.

To investigate whether striping is present in the AWS observations, we have used the level-1B format without remapping or averaging. Atkinson (2015) suggests a measure for striping via a Striping Index of the form:

$$SI = \sqrt{\frac{\overline{\sigma_{AT}^2}}{\overline{\sigma_{CT}^2}}}$$

Where AT and CT represent along track and cross track variation. A value in excess of 1 indicates the presence of striping. Although Atkinson used calibration views, this approach can also be used with the departure (or C-B) values as follows.
For a single descending half orbit of data over ice-free ocean or land comprising of 1500 scanlines (as shown in Figure 20), a Striping Index (SI) in 12 x 12 pixel boxes by computing the along track and along track variation in C-B. This gives 1340 boxes with which to estimate the SI for each channel, though in practice the optimal size of the sampling could be investigated further. In addition, no quality control has been applied, which may be important for the submm band with its strong sensitivity to hydrometeors. The SI was determined for each of the sounding channels in the three bands (50, 183, 325 GHz). The range of the SI was found to be as follows:

- Feedhorn 1 [50 GHz band]: 0.83-1.44
- Feedhorn 2 [183 GHz band]: 0.87-1.00
- Feedhorn 4 [325 GHz band]: 0.94-1.10

The error associated with the estimates is in the range 0.05 to 0.1. The channels with the largest SI in each band are shown in Figure 20. Whilst channel 5 exhibits some striping effects, for the other bands it appears small. This may be because for the humidity sounding channels the striping effect could be masked by the larger forecast error associated with these channels. Compared to other estimates of SI this maximum value found for AWS is low, e.g. Doherty et al. (2015) reports that the SI is ~2 for SNPP ATMS 50 GHz channels using a similar approach.

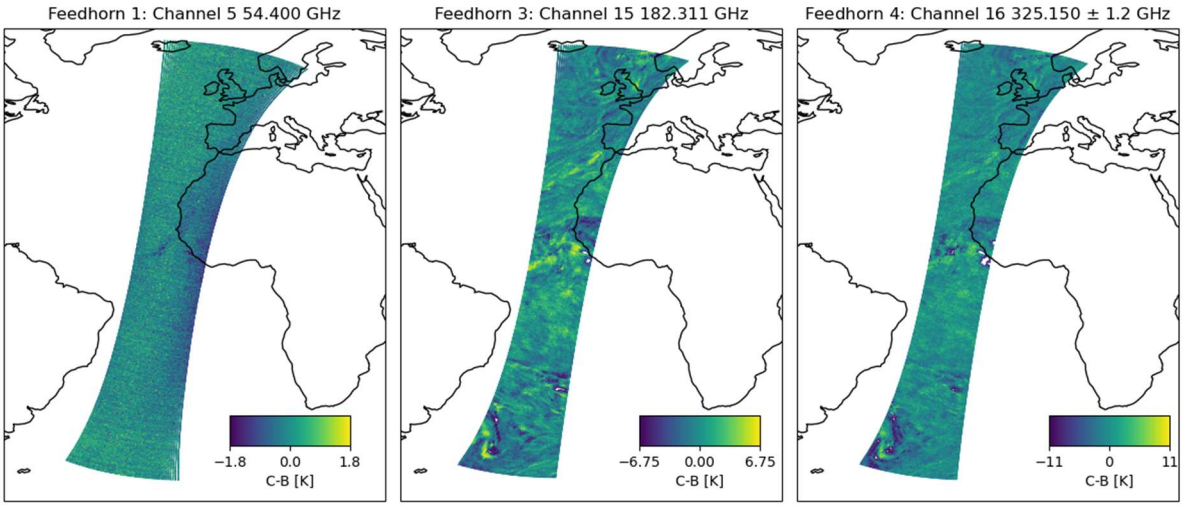

Figure 20. C-B spatial plots of part of a descending orbit for the unaveraged Level 1B data. The channels shown are those that exhibit the largest Striping Index for sounding band.

5. Timeliness of MWR/AWS data

In the context of the NWP SAF, the data reception and data timeliness are monitored for the satellite instruments typically used and assimilated in NWP. For this monitoring, the timeliness is calculated as the time elapsed between the actual observation time and the time of data base entry at either DWD or the Met Office. Up to date results which are refreshed four times daily are available via the NWP SAF web page showing:

- Traffic light type overview of the current timeliness and data reception status: Data Status | NWP SAF
- Data coverage: Data Coverage Monitoring | NWP SAF
- Data timeliness: Data Timeliness | NWP SAF

Here, we include recent results for the month of December 2025 as an illustration. Data availability and timeliness is normally very stable, but please refer to the above web pages for the current status (AWS plots will be included on the operational web pages in Q1/2026). Figure 22 displays the typical coverage of MWR/AWS data for two examples of 6-hour periods centered on 00 UTC and 18 UTC. Additionally, the plot indicates the timeliness achieved at different positions, with blue shades indicating the shortest timelines of 30-40 min. The monitoring is based on the EUMETCast data stream intended for global NWP which relies on a downlink once per orbit at Svalbard. Therefore, the timeliness is best just south of the northern polar area (on ascending node) and may even meet the very strict timeliness requirements of regional short-range NWP systems in these areas.
When looking at longer timeliness statistics, shown here in Figure 21 for December 2025 as a monthly pdf diagram, we see that 90% of the data arrive within 2h, with the maximum delay being only 2h28 and well below the typically defined maximum threshold of 3h. Therefore, most of the data arrive within typical data use cut-off times for global NWP systems which may be as low as about 2h.

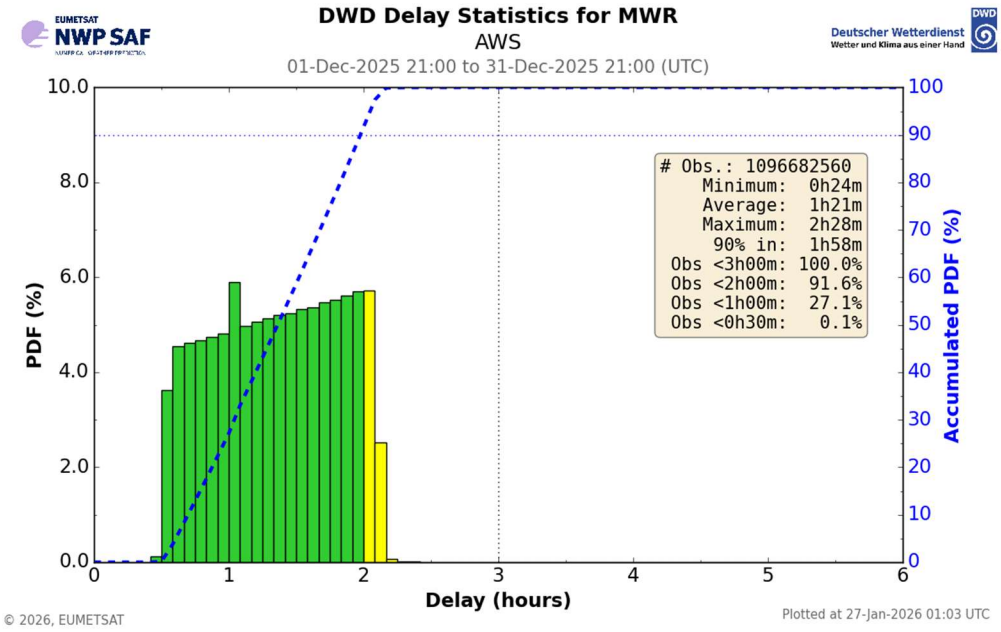

Figure 21: Overall timeliness of the MWR/AWS data received through EUMETCast in December 2025 showing the timeliness pdf and accumulated pdf. Results are based on the data entry into the DWD data base.

The timeliness as well as the number of data received are very stable in time apart from minor data gaps occurring from time to time, as shown in the timeliness timeseries in Figure 23.

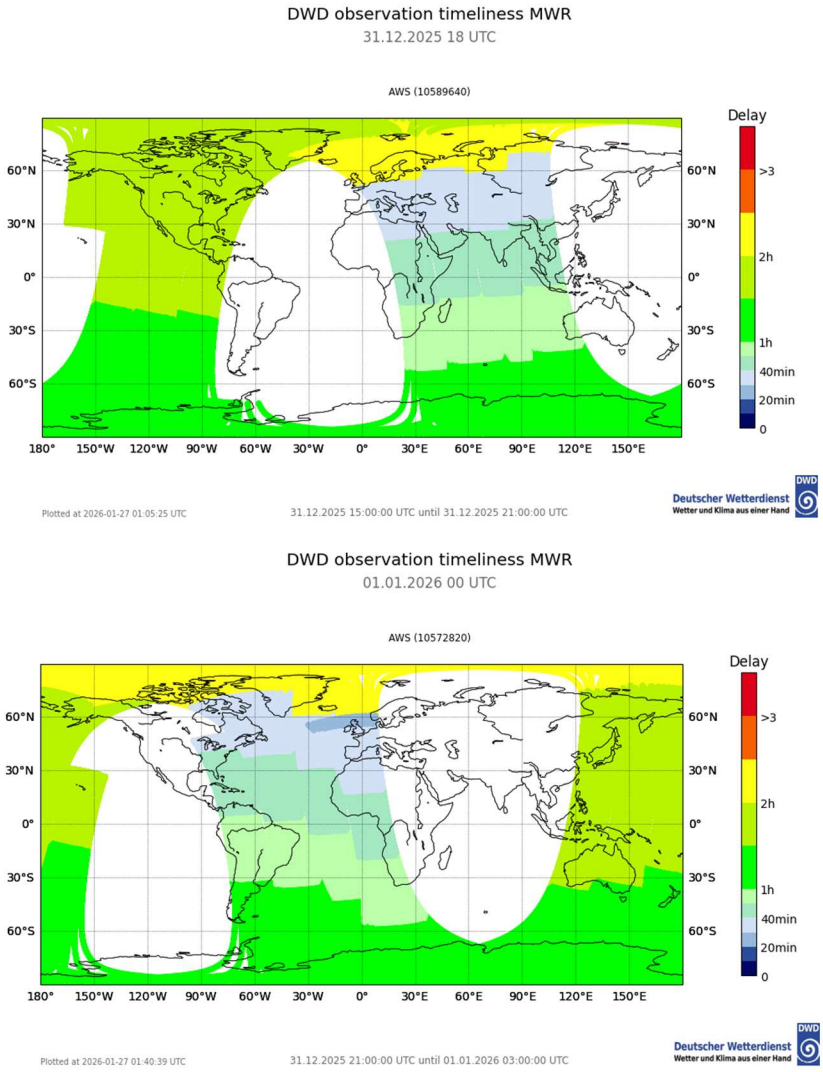

Figure 22: Examples of data coverage and its timeliness for two of the four daily 6h periods available in the NWP SAF data reception monitoring, here for the 31.12.2025 centered at 18UTC and 1.1.2026 at 00 UTC. Results are based on the data entry into the DWD data base.

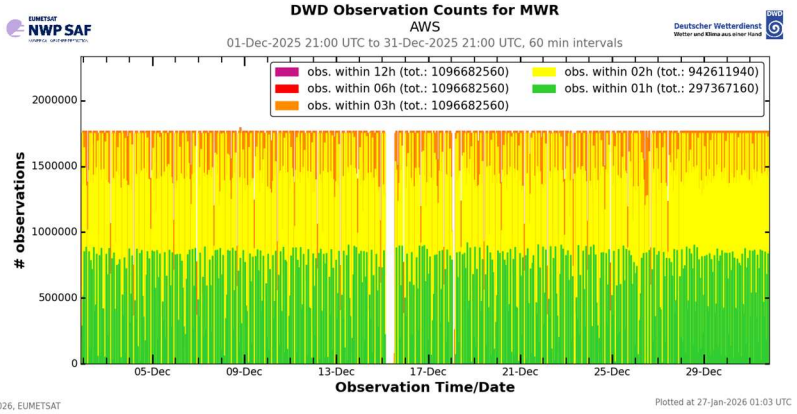

Figure 23: Timeseries of data timeliness of the MWR/AWS data for December 2025 showing the number of data points (here FOVs) received within certain timeliness windows. Results are based on the data entry into the DWD data base.

6. Forecast Impact Study

An impact study of the assimilation of AWS data in the Met Office global model was performed and the results are summarised here. The trial period was 15th May 2025 – 15th July 2025 and the control run represents the Operational Suite 7 configuration which became operational in February 2026. The other observation types used in both trial and control runs consist of all the systems available to Met Office operations in summer 2025. For instance, the other microwave sounders used are: AMSU-A/MHS (Metop-B and C), ATMS (NOAA-20 and 21), SSMIS (DMSP-18) and MWHS2 onboard FY3D.
The quality control used for the assimilation of the AWS data differs from the monitoring activity and follows the all-sky approach outlined in Candy & Migliorini (2021). This approach uses 1D-Var retrievals of ice water path and liquid water path at each observation location to inflate the observation errors in cloudy scenes. Scenes identified as containing precipitation are rejected prior to the 1D-Var step.
Temperature sounding channels with low surface to space transmittance are assimilated over land and sea, with the other channels used only over sea (data usage is shown in Table 3). Table 3 also shows the typical amount of data from each channel after the removal of precipitation scenes, and the surface type. The final step in the process is to perform spatial thinning. This is a standard practice in data assimilation and is applied, in part, to reduce spatial error correlations between observations. The amount of thinning applied for this initial trial was set at 125 km, which is the value used in the extratropical regions for the ATMS instruments. An example coverage plot for six hours of data assimilated from channel 5 is shown in Figure 24.

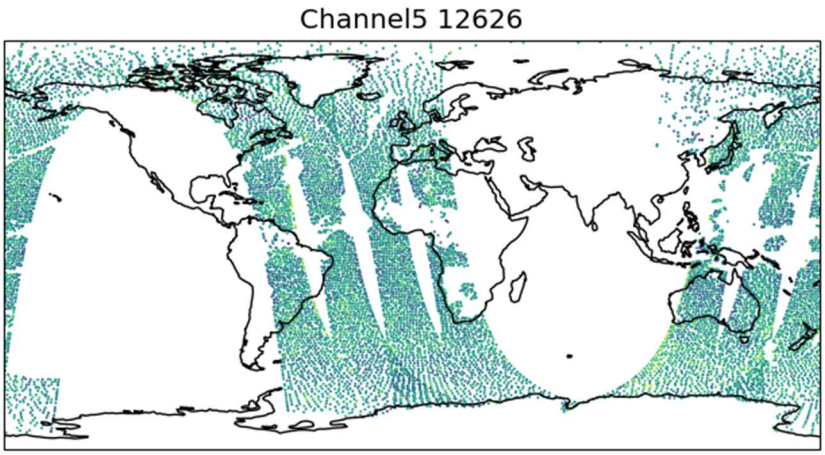

Figure 24. Spatial coverage for 6 hours of data (one assimilation cycle) for AWS Channel 5. Quality control and thinning have been applied.

Channel	Usage		Average Number of Observations Per cycle (after thinning).
	Sea	Land & Sea-Ice	
1: 50.300	N	N	0
2: 52.800	Y	N	7651
3: 53.246	Y	N	7651
4: 53.596	Y	N	7651
5: 54.400	Y	Y	11581
6: 54.940	Y	Y	11581
7: 55.500	Y	Y	11581
8: 57.290	Y	Y	11581
9: 89.000	N	N	0
10: 165.500	N	N	0
11: 176.311	Y	N	7656
12: 178.811	Y	N	7656
13: 180.311	Y	N	7656
14: 181.511	Y	N	7656
15: 182.311	Y	N	7656
16: 325.150±1.2	Y	N	7656
17: 325.150±2.4	Y	N	7656
18: 325.150±4.1	Y	N	7656
19: 325.150±6.6	Y	N	7656

Table 3: Data usage over different surface types and the average number of observations assimilated per 6-hour cycle for each AWS channel.

The verification results of the AWS trial compared to the control run is shown in Figure 25 (using ECMWF analyses as a source of verification truth). The results are presented in the standard Met Office scorecard. This shows the impact of the trial on various forecast parameters (y-axis) according to forecast time (x-axis) out to 5 days (T+144 hours). Green elements of the scorecard indicate improved forecast errors, whilst blue elements represent

degradations. The results show that this initial use of AWS data improves the wind forecasts in both Northern and Southern Extratropical regions out to 2 days. Improvements can also be seen in the Temperature fields, notably in the SH at 500 hPa. Overall, the mean change in all variables of the score card is found to have improved by 0.16%, which is considered statistically significant based on the variation in scores found in standard trials of this type. This is a very encouraging result for the first use (in the Met Office) of data from AWS. Further tuning of the channel selection and data thinning is likely to result in a higher impact beyond this first study.

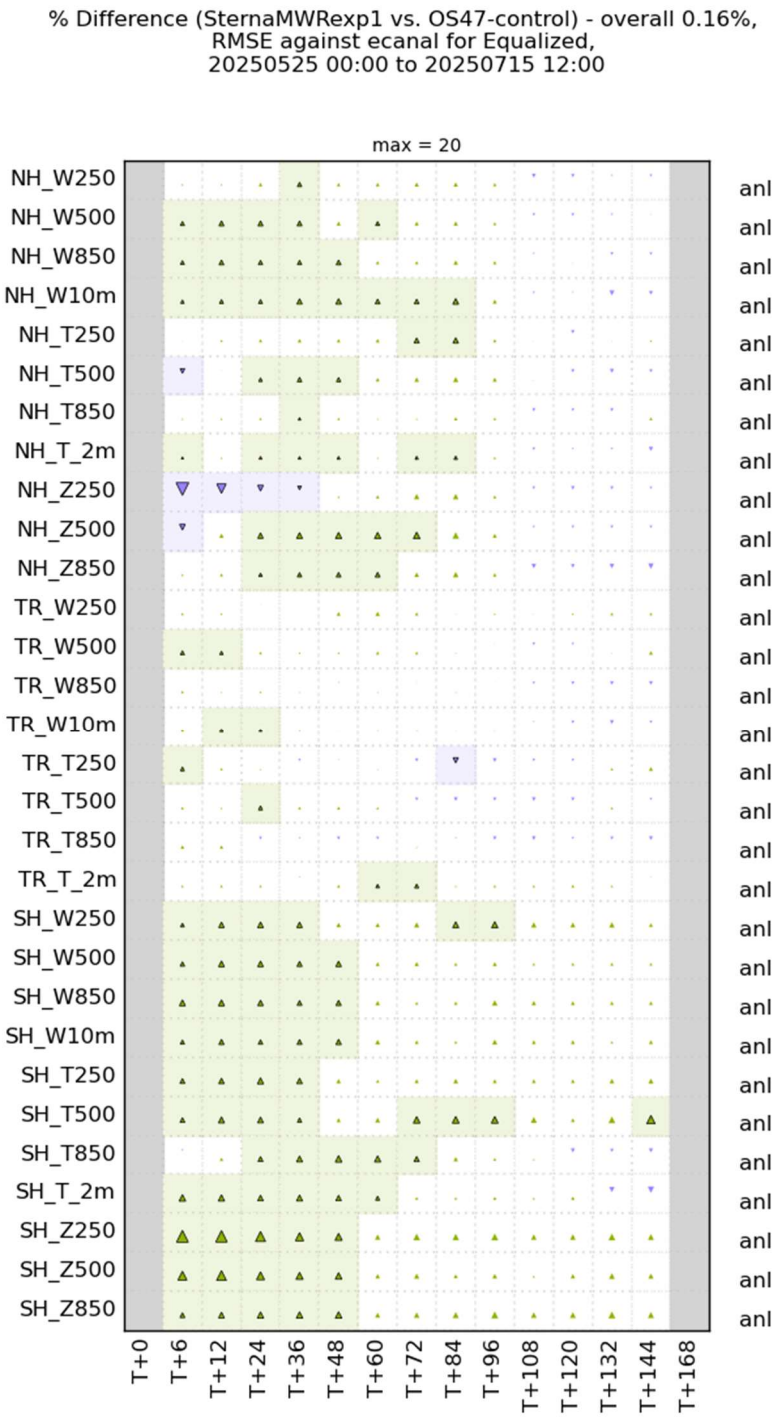

Figure 25. The forecast impact score card for the Met Office impact trial of AWS observations. NH, TR and SH denote Northern Hemisphere, Tropical and Southern Hemisphere latitude bands.

7. Conclusions

The new MWR instrument on the AWS satellite has been launched mid August 2024 with instrument CalVal, data processing and dissemination being set up to reach operational dissemination via EUMETCast by 20 April 2025.
For this report, the instrument data quality has been evaluated using equivalent brightness temperatures calculated with RTTOV from very short-range forecasts of two independent NWP model systems, namely the Met Office Unified model and DWD operational ICON model, as references. The results based on the two independent models lead to very consistent conclusions regarding the bias and noise behaviour of the instrument in the different frequency ranges.
The statistical results show some biases of measured radiances (converted to brightness temperatures) versus the equivalent model brightness temperatures. While an NWP model comparison does not allow an estimate of the absolute bias value, and indeed the results for both models differ slightly, the independent results clearly and consistently indicate a scan angle dependence of the biases. This scan angle bias is strongest in the 183 GHz band channels and is likely linked to the presence of some debris in the corresponding feedhorn as was analysed by ESA. The scan bias patterns are very stable in time and bias correction approaches as typically used in NWP can correct such biases and are also able to correct small variations that may very occasionally occur in time. The resulting residuals are very small and stable in time.
The standard deviation of observations minus model values, based on averaged MWR observations representing scales comparable to the effective resolution of the global NWP models, the instrument noise, being a component of the standard deviation of observations minus model values, can be assessed. For the 3*3 and 5*5 FOV averages used in the MetOffice and DWD statistics, respectively, this noise component is around or below 0.1-0.3 K for the channels in the 50 GHz band. This is slightly above the corresponding values for ATMS at a comparable resolution. The only MWR/AWS channel with a noticeably higher noise is channel 8 at 57.29 GHz. The reason for this is understood by ESA and any follow-on instruments based on the MWR/AWS design can be improved accordingly.
For the channels of the 183 GHz and the new 325 GHz bands the size of the bias corrected observation minus model background standard deviations are higher and in the range 0.8-2.0 K, but these bands also include a typically higher representativeness error component inherent in the NWP based comparisons. The magnitude of the diagnosed noise is again in line with those seen for corresponding instruments and the evaluation shows them to be very stable in time for all the channels in the different frequency bands.

The data availability and timeliness via the EUMETCast dissemination system is very stable with 90% of the global dataset arriving within 2h and typically all data within 2h30min.

The initial NWP forecast impact at the Met Office showed a very promising impact in an all-sky configuration. There is expectation that the impact can be improved further thorough tuning of the quality control and improved estimate of the Rmatrix.

Therefore, these very good evaluation results show that the new design of the small MW sounding instrument MWR on AWS provides high quality measurements with excellent reliability. This enables these new data to be used for operational weather forecasting systems and the instrument provides a very good basis for the planned EPS-Sterna satellite configuration to be flying several instruments of this design in complementary polar orbits.

8. References

Atkinson, N., 2014. Striping Tests for microwave sounders, Satellite Applications Tech Memo no. 17, Available from the author.

Bennartz, R., Thoss, A., Dybbroe, A. and Michelson, D.B., 2002. Precipitation analysis using the Advanced Microwave Sounding Unit in support of nowcasting applications. *Meteorological Applications*, *9*(2), pp.177-189.

Buehler et al. (2007): "A cloud filtering method for microwave upper tropospheric humidity measurements", Atmos. Chem. Phys., 7, 5531-5542.

Candy, B. and Migliorini, S. (2021). The assimilation of microwave humidity sounder observations in all-sky conditions. *Quarterly Journal of the Royal Meteorological Society*, *147*(739), pp.3049-3066.

Doherty, A., Atkinson, N., Bell, W. and Smith, A., 2015. An assessment of data from the advanced technology microwave sounder at the Met Office. *Advances in Meteorology*, *2015*(1), p.956920.

Eriksson, P., Emrich, A., Kempe, K., Riesbeck, J., Aljarosha, A., Auriacombe, O., Kugelberg, J., Hekma, E., Albers, R., Murk, A. and Møller Pedersen, S. (2025). The Arctic Weather Satellite radiometer. *Atmospheric Measurement Techniques*, *18*(18), pp.4709-4729

Kalluri, S (Ed.) (2021). Satellite Microwave Sounding Measurements in Weather Prediction: A Report of The Virtual NOAA Workshop on Microwave Sounders, https://doi.org/10.25923/wkgd-pw75

F. Karbou, C. Prigent, L. Eymard and J. R. Pardo, 2005: Microwave land emissivity calculations using AMSU measurements, in *IEEE Transactions on Geoscience and Remote Sensing*, vol. 43, no. 5, pp. 948-959, doi: 10.1109/TGRS.2004.837503.

Lean, K., Bormann, N., Healy, S., English, S., Schuettemeyer, D., and Drusch, M. (2025). Assessing forecast benefits of future constellations of microwave sounders on small satellites using an ensemble of data assimilations. Quarterly Journal of the Royal Meteorological Society. 10.1002/qj.4939.

Lupu C., Geer A., Bormann N., and English S., 2016: An evaluation of radiative transfer modelling errors in AMSU-A data. European Centre for Medium-Range Weather Forecasts. Tech, Memo. 170.

Qin Zhengkun and Zou Xiaolei, 2016: Development and initial assessment of a new land index for microwave humidity sounder cloud detection. J. Meteor. Res., 30(1), 012–037, doi: 10.1007/s13351-016-5076-4

Saunders, R., Hocking, J., Turner, E., Rayer, P., Rundle, D., Brunel, P., Vidot, J., Roquet, P., Matricardi, M., Geer, A., Bormann, N., and Lupu, C. (2018). An update on the RTTOV fast radiative transfer model (currently at version 12), Geosci. Model Dev., 11, 2717–2737, https://doi.org/10.5194/gmd-11-2717-2018

Turner, E., Rayer, P. and Saunders, R., 2019. AMSUTRAN: A microwave transmittance code for satellite remote sensing. *Journal of Quantitative Spectroscopy and Radiative Transfer*, *227*, pp.117-129.

Yang, J.X., You, Y., Blackwell, W., Misra, S. and Kroodsma, R.A., 2021. Quantifying and characterizing striping of microwave humidity sounder with observation and simulation. *IEEE Transactions on Geoscience and Remote Sensing*, *60*, pp.1-13.